Experimental Evaluation of Minimum Swept-Path Control for Autonomous Reversing of Articulated Vehicles

Xuanzuo Liu[1], Anil K. Madhusudhanan[1] and David Cebon[1]

***Abstract*— This paper validates a newly devised control method for autonomous reversing of articulated vehicles called Minimum Swept Path Control (MSPC) [1], [2]. The theory in [1] can be applied to multiple trailers. The main linear optimal controller was implemented on full-sized tractor-semitrailer and B-double (twin trailer) combinations owned by Cambridge Vehicle Dynamic Consortium (CVDC). An inner-loop compensator using the PID method was developed and tuned to track the desired steer angle generated by the main controller. The experimental results are in agreement with the simulation results in [1], demonstrating that this approach can reduce the overall swept path of articulated vehicles during autonomous reversing significantly and guarantee accurate convergence to the terminal position of the manoeuvre.**

***Index Terms*— Autonomous Reversing, Articulated Vehicles, Minimum Swept Path Control, Path Following Control, Experimental Evaluation.**

I. INTRODUCTION

Heavy goods vehicles (HGVs) perform a vital role in freight transport, accounting for 73% of over-land-transported freight compared to the rail transport across the European continent [3]. Reversing articulated vehicles is challenging for drivers. In addition, to reduce carbon emissions and fuel consumption, the trend towards greater length and multiple articulation points exacerbates this difficulty [4]. Autonomous reversing systems can assist drivers to overcome this difficulty [5]–[8].

Previous research [5]–[11] was concerned with the stability and accuracy of path following in reverse, which causes large swept path width during manoeuvres. Rimmer [5]–[8] developed a path-following controller (PFC) to reduce the error between a rear-end point of Long Combination Vehicles (LCVs) and a pre-defined path. However, this control strategy caused large excursions of tractor. This results in practical limitations. For instance, these methods cannot be implemented in confined spaces such as narrow road lanes, as the sum of two maximum deviations at both sides of the desired path by using the PFC method is larger than the lane width. The maximum width of the swept path is a threshold to decide whether the vehicle units can complete their manoeuvres within the confined spaces. Compared to the PFC, a newly devised method called Minimum Swept Path Control (MSPC) [1] can reduce the maximum excursions by more than 40%, which allows vehicles to pass through the confined spaces, while guaranteeing acceptably accurate path following [1]. The theory in [1] can also be extended to LCVs.

To validate the MSPC, it was implemented on an experimental, full scale tractor-semitrailer and a B-double, shown in Figures 1 and 2. Two reversing manoeuvres, a lane change with continuously changing curvature and a roundabout, were performed to test the performance of the controller in transient and steady state conditions.

Fig. 1. Tractor-semitrailer test vehicle. Distances shown between the front axle and the hitch point for the tractor, and hitch to second rear axle for the semitrailer.

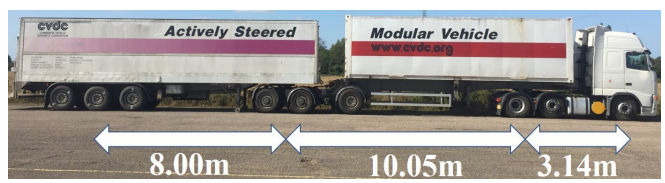

Fig. 2. B-double test vehicle. Distances shown between the front axle and the hitch point for the tractor, hitch to hitch point for the B-link trailer, and hitch to second rear axle for the semitrailer.

The outline of the paper is as follows: Section 2 describes the implementation of MSPC on the test vehicles and Section 3 briefly describes the vehicle dynamics system for the development of control system. The experimental and simulation results are compared in Section 4 and the main conclusions and future work are in Section 5.

II. VEHICLE MODEL

The vehicle dynamics model in [1] was extended for multiple trailers. For simplicity, the trailer units were assumed to have one 'equivalent axle' in each axle group. The longitudinal speed of tractor, u_0, was assumed to be constant. The main ordinary differential equations (ODEs) for the tractor are as follows:

$$m_0(\dot{v}_0 + u_0\Omega_0) = F_{f_0}cos(\delta) + F_{r_0} + Y_{H_0}, \tag{1}$$

$$I_{z_0}\dot{\Omega}_0 = F_{f_0}cos(\delta)a_0 - F_{r_0}b_0 - Y_{H_0}(b_0 + c_0), \tag{2}$$

[1]Xuanzuo Liu, Anil K. Madhusudhanan and David Cebon are with the Department of Engineering, University of Cambridge, Trumpington Street, Cambridge, CB2 1PZ, U.K. (Corresponding author is Xuanzuo Liu)
e-mail: xzl20@cam.ac.uk; ak2102@cam.ac.uk; dc@eng.cam.ac.uk

where δ is the steer angle of the tractor. m_0 and I_{z_0} denote the mass and yaw moment of inertia of the tractor. v_0 and Ω_0 are the lateral and yaw velocities of the Centre of Mass (C.o.M.) of the tractor. $\dot{v}_0$ and $\dot{\Omega}_0$ are the first derivatives of v_0 and Ω_0, respectively. a_0, b_0 and c_0 indicate the distances between the front and rear axles, the C.o.M. and the hitch point of the ith trailer as shown in Figure 3. Y_{H_0} is the lateral force of the first hitch point between the first trailer unit and the tractor. F_{f_0} and F_{r_0} are the lateral tyre forces of the front and rear axle of the tractor. The main ODEs for the trailers are as follows:

$$I_{z_i}\dot{\Omega}_i = -Y_{H_i}(a_i + b_i + c_i) + m_i(\dot{v}_i + u_i\Omega_i)a_i - F_{r_i}(a_i + b_i), \tag{3}$$

$$Y_{H_{i-1}} = (Y_{H_i} + F_{r_i} - m_i(\dot{v}_i + u_i\Omega_i))cos(\Gamma_i) + (X_{H_i} - m_i(\dot{u}_i - v_i\Omega_i))sin(\Gamma_i), \tag{4}$$

$$X_{H_{i-1}} = -(Y_{H_i} + F_{r_i} - m_i(\dot{v}_i + u_i\Omega_i))sin(\Gamma_i) + (X_{H_i} - m_i(\dot{u}_i - v_i\Omega_i))cos(\Gamma_i), \tag{5}$$

where m_i and I_{z_i} are the mass and yaw moment of inertia of the ith trailer. u_i, v_i and Ω_i are the longitudinal, lateral and yaw velocities of the C.o.M. of the ith trailer. $\dot{u}_i$, $\dot{v}_i$ and $\dot{\Omega}_i$ are the first derivatives of u_i, v_i and Ω_i, respectively. a_i, b_i and c_i denote the distances between the front and rear axles, the C.o.M. and the hitch point of the ith trailer. Γ_i is the articulation angle between the ith and $(i+1)^{th}$ vehicle units. X_{H_i} and Y_{H_i} are the longitudinal and lateral forces of the $(i+1)^{th}$ hitch point between the ith and $(i+1)^{th}$ trailer units. F_{r_i} represents the lateral tyre force of the rear axle of the ith trailer. $i \in [1, n]$ and n is the total number of the trailer units.

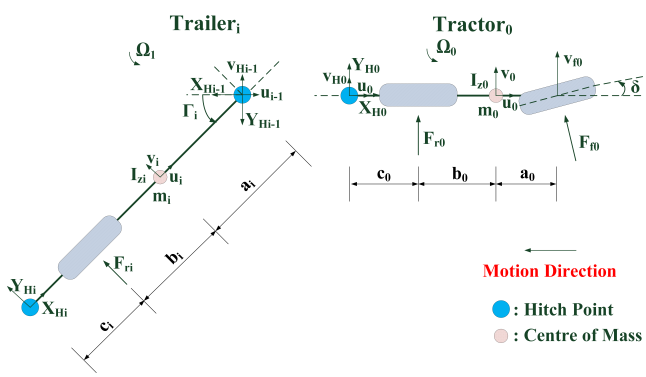

Fig. 3. Vehicle velocity and force analysis.

Specifically, for this paper experiments, $n = 1$ for the tractor-semitrailer model and $n = 2$ for the B-double model. The linearisation to build the state-space model is the same as in [1].

III. IMPLEMENTATION OF THE AUTONOMOUS REVERSING SYSTEM

A. System Architecture

The overall system architecture is shown in Figure 4. A dual antenna inertial and GPS navigation system [13] was mounted at the rear of the semitrailer to determine the speed, position and headings of the semitrailer and communicate these signals to the main controller via a Controller Area Network (CAN) bus. A GPS base station [14] was used on the testing field to improve the measurement accuracy by providing the Real Time Kinematic (RTK) differential corrections via the radio modem. Calibrated articulation angle sensors [15], [16] were installed on the kingpin of the trailers to measure the articulation angles between the vehicle units. The analogue articulation angle signals were converted to CAN signals through a low pass filter and an analogue-digital converter [17] and were fed into the MSPC subsystem. A string potentiometer [18] was attached to the front left steering radius arm and calibrated to measure the effective 'single-track' average steer angle. This analogue signal was low-pass filtered, digitised and fed into the steer angle tracking subsystem. The relationship between the hand wheel angle and the effective single-track average steer angle was measured. This relationship was non-linear due to steering system imperfections (e.g. backlash). The articulation angle sensors and string pot were zeroed at the start of each test to offset the small drifts. A steering robot [19] was used to follow the hand wheel angle demand calculated by the steer angle tracking subsystem. The steering robot was configured to follow a signal on an external CAN bus with a short delay at a corner frequency of 25 Hz. The tractor speed was obtained from CAN messages read from its FMS port. The real time system was run on an xPC for the implementation on the semitrailer and on a dSpace AutoBox [20] for the implementation on the B-double. The xPC was a dual-core target PC without operating systems and had two Softing AC2-PCI dual CAN bus cards [21] in the PCI slots. The AutoBox had a DS1007 dual-core board (2.0GHz) and a CAN interface board. Both the xPC and Autobox were connected to a laptop via an Ethernet cable.

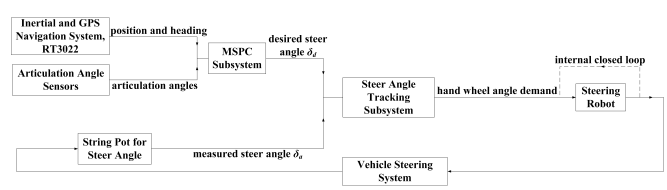

Fig. 4. Architecture of the autonomous reversing system.

B. MSPC subsystem

The MSPC controller has the structure shown in Figure 5. The control method in [1] was extended for multiple trailers and was formulated as follows:

$$\delta_d = \delta_e + K_{y_{ra}}y_{ra} + K_{\theta_{ra}}(\theta_p - \theta_{ra}) + \sum_{i=1}^{n} K_{\Gamma_i}(\Gamma_{ie} - \Gamma_i), \tag{6}$$

where δ_d is the demanded steer angle control input. δ_e and Γ_{ie} are the equilibrium steer and articulation angles, calculated from the future equilibrium state. θ_p is the heading

of the reference path and θ_{ra} is the heading of the semitrailer. Γ_i is the real-time articulation angle of the ith trailer. For the tractor-semitrailer combination, $n = 1$ and Γ_1 is the articulation angle between the tractor and semitrailer. In the case of B-double, $n = 2$. Γ_1 denotes the articulation angle between the tractor and B-link trailer, and Γ_2 refers to the articulation angle between the B-link trailer and semitrailer. y_{ra} denotes the lateral offsets of the rear axle of the semitrailer. $K_{y_{ra}}$, K_{ra} and K_{Γ_i} are the corresponding control gains for the rear lateral offset error, the heading angle error, and the articulation angle error, respectively. The gains were determined using the linear-quadratic-regulator theory [22] with appropriate weights for the lateral offsets of the front axle of the tractor, W_{fa}, and the rear axle of the semitrailer, W_{ra}. The cost function, J, is defined as follows:

$$J = \int_0^{\infty} (W_{ra} y_{ra}^2 + W_{fa} y_{fa}^2 + \delta_d^2)\, dt, \tag{7}$$

where y_{fa} denotes the lateral offsets of the front axle of the tractor.

The weight selection criteria and optimisation of the preview distance were described thoroughly in [1]. For this implementation, the optimal weights, $W_{fa} = 1$ and $W_{ra} = 0.1$, were found.

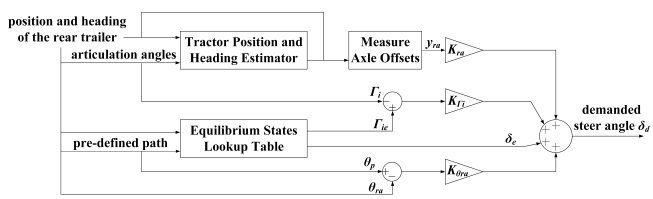

Fig. 5. MSPC subsystem.

C. Steer angle tracking subsystem

The steer angle tracking subsystem enables the actual steer angle, δ_a, to follow the demanded steer angle, δ_d, in order to improve the reversing performance. The system structure is a combination of feedforward and PID control, as shown in Figure 6.

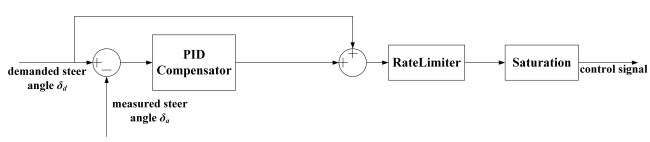

Fig. 6. Steer angle tracking subsystem.

The transfer function, $H(z)$, for the discrete-time parallel PID compensator is as follows:

$$H(z) = K_p + K_I * \frac{T_r}{z-1} + K_D * \frac{C_D}{1 + C_D * \frac{T_r}{z-1}} \tag{8}$$

where T_r is the real-time processor's sampling time. K_P, K_I and K_D are the proportional, integral and derivative gains respectively. C_D is the coefficient for the derivative filter.

The output of PID compensator was rate limited and saturated by the known physical limitations of the tractor steering system. Then it was converted to the hand wheel angle based on the measured relationship between the hand wheel angle and the effective 'single-track' average steer angle. The demanded hand wheel angle was sent to the steering robot.

A saturated ramp signal for the steer angle demand, δ_d, was used to tune the PID controller experimentally. The steering robot was set to follow the external signal. Firstly, the gains, K_P, K_I and K_D, were set to zero, and the raw steady state offset between the input signal and the measured steer angle, δ_a, was measured and plotted in Figure 7. Then, K_I and K_D remained zero, and K_P was increased gradually to reduce the steady state offset until there was insignificant effect on the steady state error. After tuning K_P, K_D remained unchanged and K_I was increased independently to eliminate the remaining steady state error. Lastly, K_D was increased slightly to improve the settling time and stability. The measured steering angle using the tuned PID gains was superimposed in Figure 7.

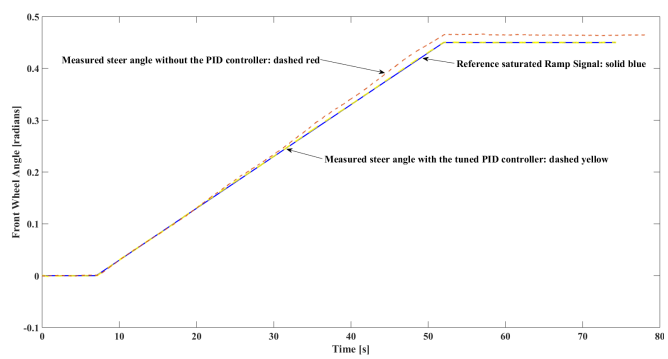

Fig. 7. Measured steering angle with and without the PID controller.

D. Testing parameters

The test vehicle geometry is shown in Figure 8 and the vehicle parameters are outlined in Tables I to III. The 'equivalent wheelbases' of the trailers were calculated using the Winkler approach [12]. The gains for the MSPC controller and PID compensator are shown in Tables IV and V. The real-time processor's sampling time, T_r, was 0.01s. The tractor speed was about 1m/s.

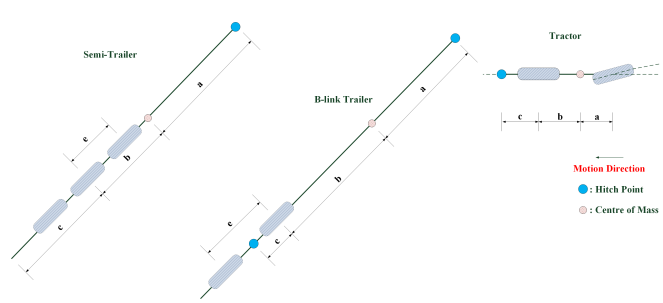

Fig. 8. Vehicle diagram showing dimensions of the vehicle units.

TABLE I

TRACTOR UNIT PARAMETERS.

Parameter	Symbol	Value	Unit
Distance from the front axle to the centre of gravity	a	1.416	m
Distance from the rear axle to the centre of gravity	b	2.684	m
Distance from the rear axle to the hitch	c	-0.96	m
Number of axles	n_a	2	

TABLE II

B-LINK TRAILER PARAMETERS.

Parameter	Symbol	Value	Unit
Distance from the front hitch point to the centre of gravity	a	4.527	m
Distance from the first rear axle to the centre of gravity	b	4.773	m
Distance from the first rear axle to the rear hitch point	c	0.75	m
Number of axles	n_a	2	
Axle spacing	e	1.45	m
Equivalent wheelbase	l_{eff}	10.077	m

TABLE III

SEMI-TRAILER PARAMETERS.

Parameter	Symbol	Value	Unit
Distance from the front hitch point to the centre of gravity	a	5.66	m
Distance from the second rear axle to the centre of gravity	b	2.34	m
Distance from the second rear axle to the rear-end	c	3.5	m
Number of axles	n_a	3	
Axle spacing	e	1.43	m
Equivalent wheelbase	l_{eff}	8.17	m

TABLE IV

GAINS FOR THE MSPC CONTROLLER.

Parameter	$K_{y_{ra}}$	$K_{\theta_{ra}}$	K_{Γ_1}	K_{Γ_2}
MSPC gains for the tractor-semitrailer	1.05	14.41	8.54	
MSPC gains for the B-double combination	-1.05	-24.79	11.27	-36.23

TABLE V

GAINS FOR THE PID COMPENSATOR.

Parameter	K_P	K_I	K_D	C_D
PID gains	1.00	0.67	0.01	100

IV. EXPERIMENTAL RESULTS

A. Steer angle tracking

Figure 9 shows the steer angle tracking during a lane change manoeuvre. The solid blue line represents the measured steer angle, δ_a, and the dashed red line denotes the demanded steer angle, δ_d, as shown in Figure 9. The measured steer angle, δ_a, is in a good agreement with the MSPC control output, δ_d. With the aid of the tracking subsystem, the tractor's front wheel was actuated to follow the demanded steer angle calculated by the main MSPC controller.

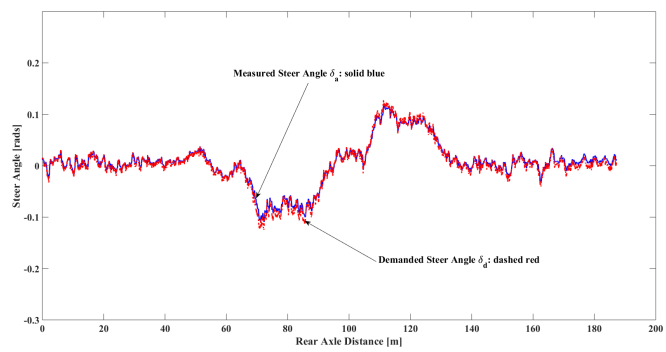

Fig. 9. Steer angle tracking during a lane change manoeuvre.

B. Lane change manoeuvre for the tractor-semitrailer case

Figure 10 shows the target path and test vehicle paths using the MSPC method and baseline PFC method, during a lane change manoeuvre for the tractor-semitrailer case. The tractor and semitrailer travelled backwards from right to left. Both the PFC and MSPC methods enabled the rear trailer to follow the desired path and ultimately converge to the terminal position. To understand the difference between the MPSC method and the baseline PFC method, Figure 11 shows the lateral offsets from the nominal path in the two approaches. In the MSPC case, the overall swept path width was reduced by more than 50% compared to the baseline PFC case.

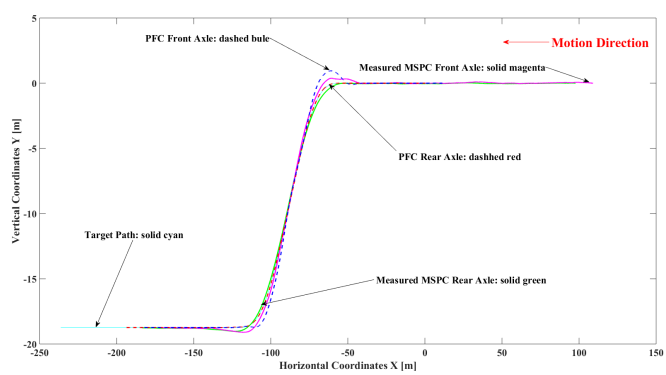

Fig. 10. Lane change manoeuvre for tractor-semitrailer.

C. Roundabout manoeuvre for the doubly-articulated vehicle case

Figure 12 shows the target path and the test vehicle paths using the MSPC method and the baseline PFC method during

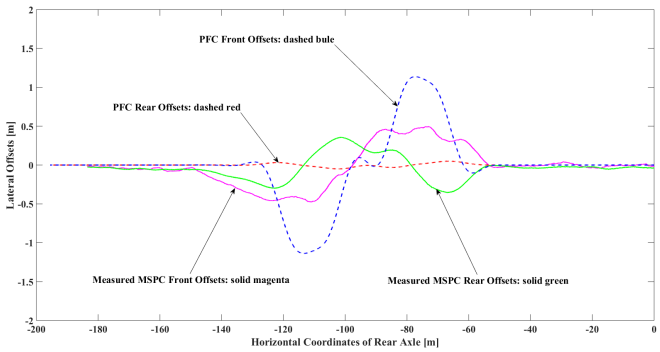

Fig. 11. Comparison of the lateral offsets during the lane change manoeuvre for tractor-semitrailer.

a roundabout manoeuvre for the B-double combination. The test vehicle still moves in the same direction. As for using the PFC method, the 'equivalent rear axle' of the rear trailer is able to track the path with small deviations, but this causes large excursions from the nominal path for the front axle of the tractor. In contrast, the MSPC allows the rear trailer to deviate from the desired path and go slightly inwards, in order to pull the other parts of the vehicle closer to the desired path and reduce the offsets. The lateral offsets comparison for the roundabout manoeuvre is shown in Figure 13. The PFC front offsets dominate both sides of the desired path. The MSPC tracking errors of the rear trailer are acceptable during the manoeuvre, not exceeding the negative maximum excursion of the PFC front offsets. The overall swept path using the MPSC method is reduced by about 40%, compared to the baseline PFC method.

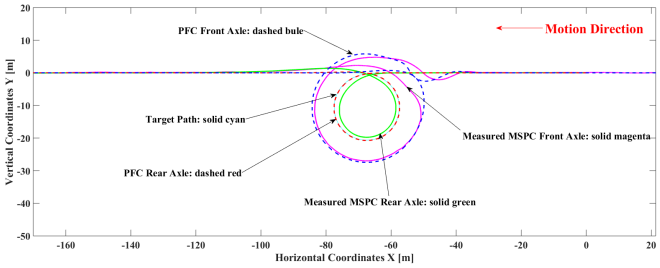

Fig. 12. Roundabout manoeuvre for B-double.

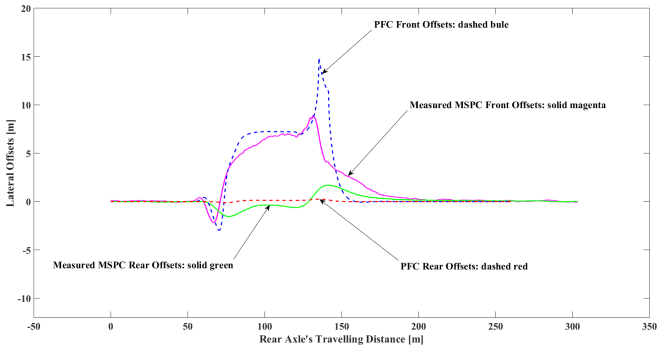

Fig. 13. Comparison of the lateral offsets during the roundabout manoeuvre for B-double.

V. CONCLUSIONS AND FUTURE WORK

This paper presents the experimental evaluation of the MSPC-based autonomous reversing of articulated vehicles. The tests validate the main theory in [1] and extend its application to doubly-articulated trailers. The experimental results show that the controller exhibits good real-time performance, reducing the overall swept path width by more than 40%, compared to the path following methods [5]–[8].

VI. ACKNOWLEDGEMENTS

This work is partially supported by the China Scholarship Council, Volvo Trucks and the Cambridge Vehicle Dynamics Consortium (CVDC). At the same time of writing the members of the CVDC are: Volvo Trucks, ABD, Horiba-MIRA, Goodyear, Haldex, IPG, Brigade Electronics, Denby Transport and SDC trailers. The authors would like to acknowledge Leo Laine from Volvo Trucks and Terry Stocks from CVDC for their collaboration and contributions to the research.

REFERENCES

[1] X. Liu, A. K. Madhusudhanan and D. Cebon, "Minimum Swept-Path Control for Autonomous Reversing of a Tractor Semi-Trailer", *IEEE Transactions on Vehicular Technology*, vol. 68, no. 5, pp. 4367-4376, 2019.

[2] X. Liu and D. Cebon, "A Minimum Swept Path Control Strategy for Reversing Articulated Vehicles," in *the 29th IEEE Intelligent Vehicles Symposium, IV18*, Changshu, China, 2018, pp. 1962-1967.

[3] European Automobile Manufacturers Association, "Trucks, Vans and Buses", https://www.acea.be/automobile-industry/trucks.

[4] I. Knight, W. Newton, A. McKinnon, et al., "Longer and/or Longer and Heavier Goods Vehicles (LHVs) a Study of the Likely Effects if Permitted in the UK: Final Report", Department for Transport (DfT).

[5] A. J. Rimmer, "Autonomous reversing of multiply-articulated heavy vehicles", Department of Engineering, University of Cambridge, Dissertation submitted for the degree of Doctor of Philosophy, 2014.

[6] A. J. Rimmer and D. Cebon, "Theory and Practice of Reversing Control on Multiply-Articulated Vehicles", *Proceedings of the Institution of Mechanical Engineers, Part D: Journal of Automobile Engineering*, vol. 230, no. 7, pp. 899-913, Aug. 2015.

[7] A. J. Rimmer and D. Cebon, "Planning Collision-Free Trajectories for Reversing Multiply-Articulated Vehicles", *IEEE Transactions on Intelligent Transportation Systems*, vol. 17, no. 7, pp. 1998-2007, Jul. 2016.

[8] D. Cebon and A. J. Rimmer, "Implementation of Reversing Control on a Doubly Articulated Vehicle", *Journal of Dynamic Systems, Measurement and Control*, vol. 139, no. 6.061011, Apr. 2017.

[9] H. Ishimoto, T. Tsubouchi, and S. Sarata, "A Practical Trajectory Following of an Articulated Steering Type Vehicle", in *Proceedings of the Conference on Field and Service Robotics*, Canberra, Australia, 1997.

[10] C. Pradalier and K. Usher, "Robust trajectory tracking for a reversing tractor trailer", *Journal of Field Robotics*, vol. 25, no. 67, pp. 378399, Jun. 2008.

[11] S. Sekhavat, F. Lamiraux, J. P. Laumond, et al., "Motion planning and control for Hilare pulling a trailer: experimental issues", in *Proceedings of International Conference on Robotics and Automation (ICRA)*, Albuquerque, New Mexico, 1997, vol. 4, pp. 33063311.

[12] C. B. Winkler, "Simplified Analysis of the Steady-State Turning of Complex Vehicles", *Vehicle System Dynamics*, vol. 29, no. 3, pp. 141-180, Mar. 1998.

[13] Anon., *GNSS-aided Inertial Measurement Systems: User Manual*, Oxford Technical Solutions Limited.

[14] Anon., *GPS-Base User Manual*, Oxford Technical Solutions Limited.

[15] V.S.E. Vehicle Systems Engineering Homepage, Available from: https://www.v-s-e.com/.

[16] Anon., *Product information ETS for trailers*, Vehicle Systems Engineering.

[17] Anon., *Application-specific PCAN-MicroMod Motherboard: User Manual*, PEAK-System Technik GmbH.
[18] Anon., *Standard Series: PA Series Analog Position User Guide*, UniMeasure.
[19] Anon., *Steering Robot SR Series User Guide*, Anthony Best Dynamics Limited.
[20] Anon., *DS1007 Hardware Installation Configuration Guide*, dSPACE GmbH.
[21] Anon., *CAN-ACx-PCI: Hardware User Manual*, Softing Industrial Automation GmbH.
[22] B. D. O. Anderson and J. B. Moore, *Linear optimal control*. Englewood Cliffs, NJ: Prentice-Hall, 1971.